Brazilian Journal of Medical and Biological Research (2014) 47(7): 567-575, http://dx.doi.org/10.1590/1414-431X20143522
ISSN 1414-431X

Modeling pulmonary fibrosis by abnormal expression of telomerase/apoptosis/ collagen V in experimental usual interstitial pneumonia

E.R. Parra[1], M.S. Pincelli[1], W.R. Teodoro[2], A.P.P. Velosa[2], V. Martins[1], M.P. Rangel[1], J.V. Barbas-Filho[1] and V.L. Capelozzi[1]

[1]Departamento de Patologia, Faculdade de Medicina, Universidade de São Paulo, São Paulo, SP, Brasil
[2]Disciplina de Reumatologia, Faculdade de Medicina, Universidade de São Paulo, São Paulo, SP, Brasil

Abstract

Limitations on tissue proliferation capacity determined by telomerase/apoptosis balance have been implicated in pathogenesis of idiopathic pulmonary fibrosis. In addition, collagen V shows promise as an inductor of apoptosis. We evaluated the quantitative relationship between the telomerase/apoptosis index, collagen V synthesis, and epithelial/fibroblast replication in mice exposed to butylated hydroxytoluene (BHT) at high oxygen concentration. Two groups of mice were analyzed: 20 mice received BHT, and 10 control mice received corn oil. Telomerase expression, apoptosis, collagen I, III, and V fibers, and hydroxyproline were evaluated by immunohistochemistry, *in situ* detection of apoptosis, electron microscopy, immunofluorescence, and histomorphometry. Electron microscopy confirmed the presence of increased alveolar epithelial cells type 1 (AEC1) in apoptosis. Immunostaining showed increased nuclear expression of telomerase in AEC type 2 (AEC2) between normal and chronic scarring areas of usual interstitial pneumonia (UIP). Control lungs and normal areas from UIP lungs showed weak green birefringence of type I and III collagens in the alveolar wall and type V collagen in the basement membrane of alveolar capillaries. The increase in collagen V was greater than collagens I and III in scarring areas of UIP. A significant direct association was found between collagen V and AEC2 apoptosis. We concluded that telomerase, collagen V fiber density, and apoptosis evaluation in experimental UIP offers the potential to control reepithelization of alveolar septa and fibroblast proliferation. Strategies aimed at preventing high rates of collagen V synthesis, or local responses to high rates of cell apoptosis, may have a significant impact in pulmonary fibrosis.

Key words: BHT experimental model; Usual interstitial pneumonia; Alveolar epithelial cell apoptosis; Telomerase activity; Collagen V; Electron microscopy

Introduction

Idiopathic pulmonary fibrosis (IPF) is an interstitial lung pneumonia of unknown cause that typically increases in prevalence with advanced age, presumably from repeated episodes of injury, repair, and scarring that lead to dramatic changes in the lung architecture and progressive respiratory failure (1). Patients with IPF have a worse prognosis than with other interstitial lung diseases, due not only to a decreased response to immunosuppressive therapies but also to the prevalence of histological patterns usually seen in usual interstitial pneumonia (UIP). There is great interest in understanding the mechanisms of tissue damage from repair and scarring, because if treatment is to be effective, one must identify these pathogenic mechanisms to avoid fibrosis and destruction of the lungs. In this context, many have debated the importance of septal inflammation (alveolitis) in the pathogenesis of UIP and have studied other mechanisms to discover those that might relate to lung repair and scarring (2,3). The repair process involves distinct stages including a regenerative phase in which the microenvironment attempts to replace apoptotic epithelial cells, new vascularization, and a fibrotic phase in which collagen fibers replace normal parenchymal tissue (4-6). However, although it is initially beneficial, failure to control the healing process can lead

Correspondence: E.R. Parra or V.L. Capelozzi, Laboratório de Histomorfometria e Genética Pulmonar, Departamento de Patologia, Faculdade de Medicina, USP, Av. Dr. Arnaldo, 455, Sala 1143, 01296-903 São Paulo, SP, Brasil. Fax: +55-11-3062-2744. E-mail: erparra20003@yahoo.com.br or vcapelozzi@lim05.fm.usp.br

Received September 17, 2013. Accepted March 6, 2014. First published online May 28, 2014.

to considerable tissue remodeling and the formation of permanent scar tissue (7).

Recently, we demonstrated (8) abnormal telomerase/apoptosis balance in alveolar epithelial cells 2 (AEC2) that reduces alveolar epithelial regenerative capacity and contributes to the early remodeling response in UIP. Reduction in the number of AEC2 results in reduced surfactant production, leading to alveolar collapse and fibrosis, which in turn involves increased collagen V synthesis, endothelial activation, and neovascularization (8-12). Thus, the telomerase/apoptosis index and collagen V synthesis in UIP offers the potential for modeling epithelial replication/apoptosis and pulmonary fibrosis. To confirm this conclusion, complementary studies in a randomized and prospective experimental model are required.

To validate the importance of the telomerase/apoptosis index and collagen V synthesis and to explore the quantitative relationships between these factors and epithelial proliferation, vascularization, and fibrosis, we studied these markers in an experimental simulated human UIP model induced in mice by 3-5-di-tert-butyl-4-hydroxytoluene (BHT).

Material and Methods

This study was carried out in strict accordance with the principles and guidelines adopted by the Brazilian College of Animal Experimentation and approved by the Ethics Committee for Animal Research of Faculdade de Medicina, Universidade de São Paulo, Brazil (Protocol No. 0960/08).

Male BALB/c mice, weighing an average of 20 g, were used in the study. The studies were performed on two groups of mice: *a*) animals that received BHT and were killed after 4 weeks (BHT group, 20 mice) and *b*) animals that received corn oil solution (control group, 10 mice).

Simulated human UIP experimental model induction

In the BHT group, 400 mg/kg BHT (Sigma Chemical Company, USA) dissolved in corn oil was injected into the animals (1.0 mL/kg of the dilution) via the intraperitoneal route. In the control group, 1.0 mL corn oil was injected similarly. The mice were placed in a ventilated Plexiglas chamber with a mixture of pure humidified oxygen and compressed air to maintain the oxygen concentration at 70%. This concentration was periodically monitored by an oxygen analyzer. Six days later, the animals were transferred to room air where they were kept for the remainder of the experiment. Food and water were available at all times.

Histology

The animals were sedated, anesthetized (20 mg/kg intraperitoneal pentobarbital sodium) and exsanguinated via the abdominal aorta. The lungs were rapidly removed, dissected, and rinsed free of blood with saline solution. Lungs were inflated *in situ* through the trachea at a pressure of 15 mmH_2O, calculated as mouse tidal volume, and fixed with 10 mL/kg (0.2 mL) buffered formalin for 6 h. The lungs were then kept in 70% ethanol for 24 h at ambient temperature. Two areas of the lungs, one peripheral and one central, were selected and embedded in paraffin, and 3-µm sections were stained with hematoxylin and eosin.

In situ detection of apoptosis and immunohistochemistry

For the *in situ* detection of apoptosis at the level of a single cell, we used an apoptotic assay with the deoxynucleotidyltranferase (TdT) method of end labeling (TUNEL; Boehringer Mannhein, Germany) (13,14). Paraffin 4-6-µm thick sections were layered onto glass slides, deparaffinized with xylene, and rehydrated with graded dilutions of ethanol. The slides were washed four times with double-distilled water for 2 min and immersed in TdT buffer (Boehringer Mannheim). Subsequently, 0.3 U/µL TdT and fluorescein-labeled dUTP in TdT buffer were added to cover the sections, and the samples were incubated in a humid atmosphere at 37°C for 60 min. For negative controls, TdT was eliminated from the reaction mixture. The sections were then incubated with an antibody specific for fluorescein conjugated to peroxidase. The staining was visualized with a substrate system in which nuclei with DNA fragmentation stained brown. The reaction was terminated by washing the sections twice in phosphate-buffered saline (PBS). The nuclei without DNA fragmentation stained blue as a result of counterstaining with hematoxylin. Positive controls consisted of rat prostate glands after castration.

Telomerase expression in AECs was detected by immunohistochemistry using a standard peroxidase technique, with Harris's hematoxylin as the counterstain. The antibody used was biotinylated rabbit polyclonal antibody. Anti-telomerase polyclonal antibody (Santa Cruz Biotechnology, Inc., USA) was incubated with tissue sections at a 1:100 dilution. The Max Polymer Novolink amplification kit (Leica, Newcastle Inc., UK) was used for signal amplification, and 3,3′-diaminobenzidine tetrachloride (0.25 mg dissolved in 1 mL 0.02% hydrogen peroxide) was used as a precipitating substrate for signal detection. The specificity of primary antibody was confirmed by appropriate reagent controls (omitting the primary antibody or substituting non-immune serum for the primary antibody in the staining protocol), which revealed no staining.

Electron microscopy

Electron microscopy was performed to confirm apoptosis of AECs in normal and scarred areas of UIP lungs in BHT-treated animals. Tissues were fixed in 2% buffered glutaraldehyde and embedded in Araldite, and thin sections were stained with uranyl acetate and lead citrate.

Biochemistry assay for collagen evaluation

To measure the quantity of collagen in the lungs, small fragments of tissue were prepared for hydroxyproline assay by the method of Bergman and Loxley (15). Tubes

containing 2 mg lyophilized material were subjected to acid hydrolysis with 6 N HCl at 100°C for 22 h. The hydrolysate was then filtered and neutralized with a saturated LiOH solution. One milliliter of the neutralized solution was diluted with isopropylic acid (Merck KGaA, Germany), oxidized with chloramin T (Sigma Chemical Co.), and then treated with Ehrlich's reagent. Analysis was carried out in duplicate. Results are reported as means and standard deviation (SD) hydroxyproline content per milligram of lyophilized tissue. Tissue weight obtained by lyophilization was not significantly different from that obtained by heating at 80°C for 24 h on a laboratory stove.

Immunofluorescence

Collagens I, III, and V in connective tissue from control and UIP lungs were identified by immunofluorescence in sections mounted on gamma methacryloxypropyltrimethoxysilane (Sigma Chemical Co.) slides. The sections were washed in xylene and dehydrated in a graded ethanol series. Antigen retrieval was done by enzymatic treatment of lungs with bovine pepsin (10,000 UTD; Sigma Chemical Co.) in 4 mg/mL acetic acid buffer, pH 2.2, for 30 min at 37°C, and subsequent incubation with 5% milk in PBS. The slides were then incubated overnight with rabbit polyclonal collagen I (1:100) and V (1:2000) and monoclonal collagen III (1:100), obtained from human placenta and produced as previously described by Miller and Rhodes (16) and Harlow and Lane (17). For negative controls, sections were incubated with fetal bovine serum instead of the primary antibody. The same tissue treatment was used for immunofluorescence detection. The sections were incubated overnight at 4°C in a humid atmosphere with the same primary antibody diluted with PBS plus 1% bovine serum albumin. Finally, the sections were incubated with fluorescein isothiocyanate-conjugated goat anti-rabbit immunoglobulins (dilution 1:50; Sigma Chemical Co.) as secondary antibody, and mounted with an aqueous mounting medium.

Histomorphometry

AEC apoptosis and telomerase expression in normal and chronic scarring areas of UIP histological patterns were assessed in 10 fields by the point-counting technique, using a 100-point grid of known area (62,500 μm^2 at 400× magnification) attached to the microscope ocular lens (18). At 400× magnification, the area in each field was calculated according to the number of points hitting connective tissue, as a proportion of the total grid area. Afterward, the number of positive cells within the connective tissue in normal septal and chronic scarring areas was counted. The fractional area of cells in apoptosis and cells expressing telomerase was determined as the number of positive cells in each field divided by the connective tissue area. The final results are reported as percentages.

Collagen fibers were quantified by optical density with the image analysis system in 10 different, randomly selected alveolar septa, as previously described by Rozin et al. (19). The results are reported as the percentage of the alveolar septal area occupied by the collagen fibers.

Interobserver comparisons were performed on 20% of the slides by two observers (MSP and ERP). The coefficient of variation for the interobserver error regarding cell count was <5%.

Statistical analysis

Analysis of variance of data (AEC apoptosis, telomerase expression, hydroxyproline, and collagen fibers) between UIP and control lungs was carried out by the Student *t*-test. A P value <0.05 was considered to be significant. Data are reported as means ± SD. All statistical procedures were carried out using the SPSS software for Windows program, release 18.0 (Released 2009. PASW Statistics for Windows, Version 18.0. SPSS Inc., IBM, USA).

Results

BHT model induces a human UIP-simulated histological pattern

The UIP histological pattern was characterized by clear evidence of alveolar collapse and chronic scarring (Figure 1A and B), typically patchy subpleural or paraseptal distribution (Figure 1A and B), and evidence of active fibrosis as fibroblastic foci (Figure 1C) with intervening normal areas.

AEC apoptosis is increased in normal and chronic scarring areas of UIP model

AEC apoptosis from control and UIP lungs, stained by TUNEL, appear as black cells in Figure 2. AEC apoptosis was more frequently observed in normal and chronic scarring areas of UIP (Figure 2B and C) compared with control lungs (Figure 2A).

Electron microscopy confirmed apoptosis in AEC types in both normal and chronic scarring areas in UIP lungs. In this situation, a large number of AEC1 were detached from the basement membrane and had markedly condensed chromatin close to the nuclear membrane. AEC1 had nuclei with chromatin condensation forming sharply circumscribed, uniformly dense, crescent-like masses that adjoined the nuclear envelope (Figure 3A). The organelles and lamellar bodies inside the AEC1 appeared to be degenerated (Figure 3B) in normal and scarring areas, with total detachment of the AEC1 (Figure 3C). In the midst of the chronic scarring areas, the denuded basement membrane could be seen with new capillaries in the septal interstitium. AEC1 were seen surrounded by myofibroblasts and collagen fibers (Figure 3D).

Table 1 shows the results of histomorphometry. AEC apoptosis was significantly increased in normal and chronic

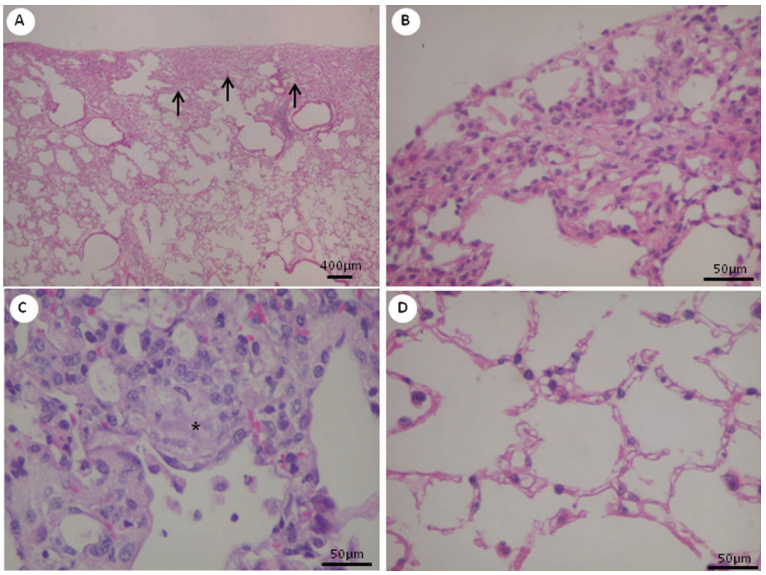

Figure 1. Histopathological changes in lung tissues at day 28. Representative H&E-stained lung tissue sections from mice treated with 3-5-di-tert-butyl-4-hydroxytoluene (BHT) are shown, with low and higher magnification views. *A*, Dense subpleural fibrosis (arrows), with collapse and obliteration of alveolar air spaces, is readily apparent. Pathological heterogeneity exemplified by dense fibrosis adjacent to relatively spared alveoli. *B*, Detail of a subpleural fibrotic area. *C*, Fibroblast focus (asterisk) is visible as a nodule of spindle cells arranged in linear fashion against a pale-staining extracellular matrix. *D*, Intervening normal alveoli.

scarring areas of UIP compared with the control lung group ($P = 0.02$, Figure 2D).

Telomerase expression is increased in normal and scarring areas of UIP model

When stained by immunohistochemistry, the nuclei of epithelial cells with telomerase expression in normal and chronic scarring areas appear as brownish/black and the cytoplasm as light brown. Numerous cells in these areas expressed telomerase when compared with the control group (Figure 4A-C).

Table 1 shows histomorphometric results. AEC2 expressing telomerase are significantly increased in normal and chronic scarring areas of UIP when compared with control lungs (Figure 4D).

Collagen V increases significantly more than collagens I and III in scarring areas of UIP

Figure 5 shows collagen fibers in the alveolar walls of control and UIP lungs stained with fluorescein by collagens I, III, and V and observed under a fluorescence microscope. In tissue sections, control lungs and normal areas from UIP lungs showed weak green birefringence of collagens I and III in the alveolar wall and collagen V in the basement membrane of alveolar capillaries, coincident with the maintenance of the architecture in both (Figure 5A-F). In contrast, the chronic scarring areas showed architectural distortion and a strong and diffuse

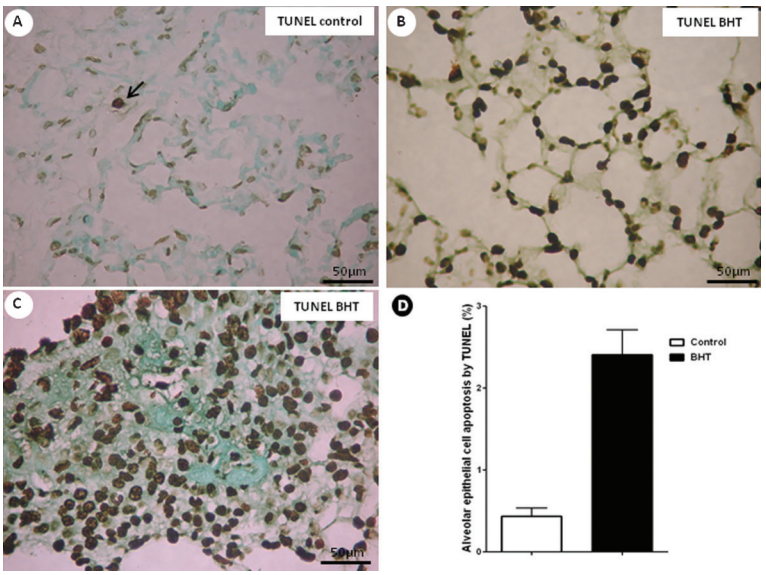

Figure 2. Apoptosis in lung tissues at day 28. Histological sections of representative TUNEL-stained lung sections from 3-5-di-tert-butyl-4-hydroxytoluene (BHT)-treated mice and a control group are shown. *A*, Control group showed sparse alveolar epithelial cells in apoptosis. *B*, *C*, BHT-treated mice exhibited numerous apoptotic alveolar epithelial cells in normal (*B*) and fibrotic (*C*) areas. *D*, Effects of BHT on alveolar epithelial cell apoptosis expression detected by TUNEL. Results are reported as area fraction (%) occupied by apoptosis in the alveolar septa. Data are reported as means ± SD, $n = 20$ for the BHT group and $n = 10$ for the control group. $P = 0.02$, BHT *vs* control (Student *t*-test).

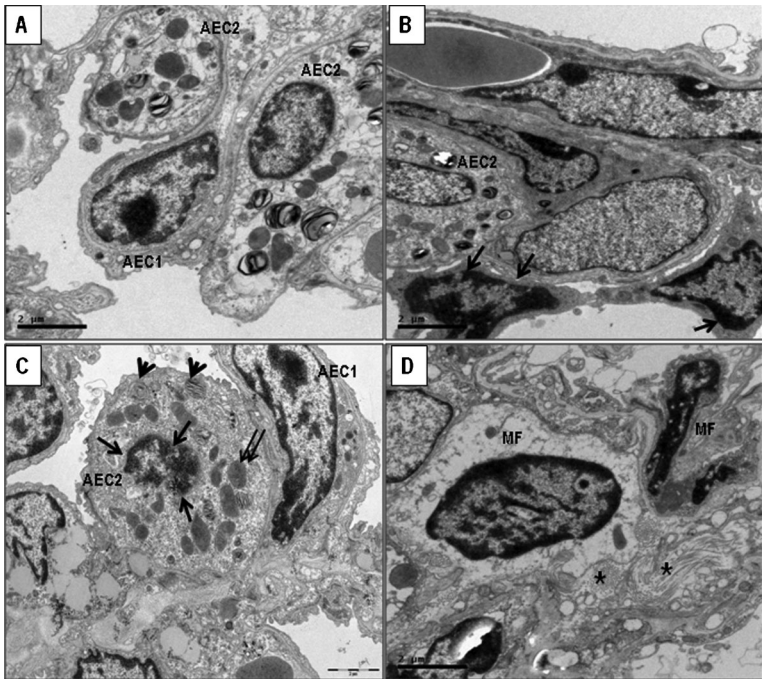

Figure 3. Representative electron microscopy of lung tissue from 3-5-di-tert-butyl-4-hydroxytoluene (BHT)-treated mice and a control group is shown in ultrathin sections. *A*, Control group showing preserved alveolar epithelial cells (AEC) along of the alveolar septa. *B*, BHT-treated mice showing AEC1 and AEC2 with marked condensed chromatin close to the nuclear membrane (*B* and *C*, arrows). *C*, The organelles (double arrows) and lamellar bodies (arrowheads) inside the AEC2 appeared to be degenerated in collapsed areas. *D*, Collagen fibers type I (asterisks) and myofibroblasts (MF) are prominent in alveolar septa of BHT-treated mice.

birefringence of collagen V (Figure 5G-I).

As expected, collagens I and III were significantly increased in scarring areas of UIP compared to control lungs. However, when compared with normal areas, collagen V increased significantly more than collagens I and III in scarring areas of UIP (Table 1 and Figure 5J).

In UIP model, collagen V and the apoptosis index are directly associated

A significant direct association was found between collagen V and AEC2 apoptosis ($r = 0.68$, $P = 0.02$).

Hydroxyproline confirms collagen increase in UIP lungs

When hydroxyproline collagen quantification was performed, a significant increase was detected in UIP compared with control lungs (Figure 5K).

Discussion

In this study, we evaluated the importance of the telomerase/apoptosis index and collagen V synthesis in experimental pulmonary fibrosis. We also explored the quantitative relationship between these factors, epithelial replication, and fibrosis in mice exposed to BHT at high oxygen concentrations. As previously demonstrated by our group (20), the BHT model resembles human UIP because of clear evidence of alveolar collapse and chronic scarring, typically patchy subpleural or paraseptal distribution, evidence of active fibrosis as fibroblastic foci, and intervening normal areas.

Because BHT accumulates predominantly in the lung (21), we found that the majority of AECs undergoing apoptosis were morphologically similar to AEC1 under high-power magnification. Further evidence was gained by electron microscopy, which demonstrated apoptotic changes in the AEC1. AEC1 apoptosis by BHT perpetuates alveolar wall denudation, considering that AEC1 division and differentiation do not re-line the alveolar wall (22). AEC2 produce surfactant and can differentiate, as required, into AEC1. However, the ability to divide must be retained by a subpopulation within the lung alveolar epithelium throughout the lifespan of any animal to replace the apoptotic AEC1 (23,24). This function has been attributed to AEC2 and may require the expression of telomerase (25-28).

In the present study, we found increased telomerase expression in a subpopulation of AEC2, suggesting that AEC2 express telomerase and are capable of proliferating and repopulating the alveolar epithelium surface, as previously described by Driscoll et al. (24). When cellular divisions shorten the telomeres in this subpopulation, the remaining telomerase-positive AEC2 may be insufficient to maintain alveolar epithelial integrity and regenerative capacity (8). The reduction in number of AEC2 results in lower production of surfactant, thus leading to alveolar collapse and fibrosis (8). Because telomerase expression is generally restricted to cells with the capacity to proliferate, UIP may result, in part, from the lack or loss of the AEC2 population in alveoli that would be capable of responding to replace the apoptotic AEC1 (8). Furthermore, proliferating AEC2 are susceptible to the cytotoxic action of oxygen,

Table 1. Summary of histomorphometric results.

Variables	Means ± SD
TUNEL (%)	
Control	0.43 ± 0.31
BHT-normal	1.68 ± 0.48
BHT-fibrotic	2.41 ± 1.35
Telomerase (%)	
Control	16.53 ± 5.23
BHT-normal	23.07 ± 1.26
BHT-fibrotic	29.25 ± 3.47
Collagen I (%)	
Control	9.49 ± 1.45
BHT-normal	18.57 ± 3.13
BHT-fibrotic	27.04 ± 12.66
Collagen III (%)	
Control	17.82 ± 2.05
BHT-normal	26.70 ± 4.39
BHT-fibrotic	34.65 ± 3.94
Collagen V (%)	
Control	17.37 ± 2.52
BHT-normal	13.63 ± 3.71
BHT-fibrotic	22.91 ± 4.77
Hydroxyproline (μg/mg)	
Control	0.47 ± 0.04
BHT	3.49 ± 2.76

The units of ''% of points'' indicate the number of points overlying the phenomena of interest divided by the total number of points overlying the connective tissue. In morphometry, this is called a point fraction and is often symbolized as Pp. Pp has been shown to approximate the area fraction or Aa (18). BHT: 3-5-di-tert-butyl-4-hydroxytoluene.

whereas dividing fibroblast cells are not (29). Interference with reepithelialization by the selective injury of epithelial cells would allow excessive proliferation of fibroblasts (fibroblastic foci). These foci are not remodeled but undergo fibrosis and are covered by regenerating AEC2, which show some atypia, and finally evolve into honeycomb features. Consequently, the renewal capacity of the AEC2 associated with its repeated division caused by oxygen injury may play an important role in the pathogenesis of experimental UIP.

The present model complements studies done in human UIP/IPF. Waisberg et al. (8) demonstrated that unaffected areas of UIP and normal lung tissue had similar densities of AEC2, but a significant minor subpopulation of AEC2 was telomerase positive and a larger population was telomerase negative. Similar findings were reported by Cronkhite et al. (30) who demonstrated that patients with IPF/UIP had a minor subpopulation of telomerase-positive myeloid cells, and hence a large population of telomerase-negative myeloid cells. The myeloid cell divisions were responsible for the shortened telomeres in this larger population. This situation might be a general occurrence in all cells in division in those UIP patients. Alder et al. (31) identified a cluster of individuals with IPF and cryptogenic liver cirrhosis, suggesting that the identified telomere shortening could contribute to what clinically appears as idiopathic progressive organ failure in the lung and the liver. Armanios et al. (32) studied families with IPF and demonstrated that telomerase was inactive, using mutations in the genes that encode telomerase components. Tsakiri et al. (33) sequenced the probands of 44 unrelated families and 44 sporadic cases of interstitial lung disease and revealed mutations in telomerase reverse transcriptase (TERT) or telomerase RNA component that result in telomere shortening over time and confer a dramatic increase in the susceptibility to adult-onset IPF. Subsequently, El-Chemaly et al. (34) identified a novel heterozygous mutation in TERT (R1084P), which results in telomerase dysfunction and short telomeres.

Our results have limitations that do not allow us to compare our experimental model to similar studies in the literature. Despite that, to our knowledge, this is the first research evaluating telomerase immunostaining in the BHT model. Liu et al. (27) and Nozaki et al. (28) of the Michigan Group demonstrated that telomerase is necessary for experimental bleomycin (BLM)-induced pulmonary fibrosis in mice. Here we studied telomerase activity in fibroblasts and evaluated telomerase immunostaining in AEC. In addition, the experimental models that we employed are different from those studies mentioned earlier. The antioxidant BHT accumulates predominantly in the lung and induces alveolar epithelial damage because of its action on AEC1 (21), which is followed by the proliferation of pulmonary parenchymal cells resembling human UIP (20,22). The cytotoxicity of BLM is the result of its capacity to fragment the DNA of AECs with consequent reduction in RNA and protein synthesis (35). BLM induces a centrilobular fibrosis, whereas in the BHT model the lesion is peripheral (21). Nevertheless, both studies have demonstrated that telomerase activity is required to avoid pulmonary fibrosis. Liu et al. (27) and Nozaki et al. (28) of the Michigan Group have also demonstrated, in tissue extracts isolated from BLM-treated rat lungs, that the injured lung fibroblast population may contain cells with increased lifespan. Subsequently, the same group demonstrated that TERT-deficient mice showed significantly reduced lung fibrosis following BLM insult. This was accompanied by a significant reduction in the expression of lung alpha smooth muscle actin, a marker of myofibroblast differentiation and increased apoptosis.

Another limitation of our study is that we found evidence of telomerase in the cytoplasm of AEC2, as indicated in Figure 4. This suggests that a nonspecific signal may have been detected and we should use a different approach to demonstrate whether it is mTert (Western blot, RT-PCR), or even to investigate other

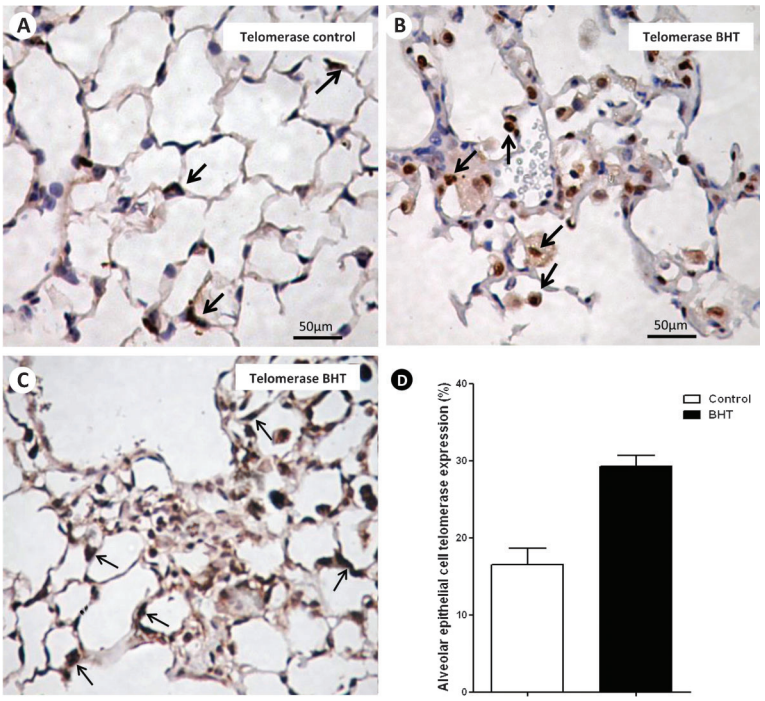

Figure 4. Representative telomerase staining of lung sections from 3-5-di-tert-butyl-4-hydroxytoluene (BHT)-treated mice and the control group at day 28 is shown in histological sections. *A*, Control group showing a few alveolar epithelial cells (AEC) expressing telomerase (arrows). *B*, *C*, BHT-treated mice exhibiting numerous alveolar epithelial cells expressing telomerase in normal and fibrotic areas (arrows). *D*, Effects of BHT on alveolar epithelial cell telomerase expression detected by immunohistochemistry. Results are reported as area fraction (%) occupied by AEC expressing telomerase in alveolar septa. Data are reported as means ± SD, n = 20 for the BHT group and n = 10 for the control group. P = 0.05, BHT *vs* control (Student *t*-test).

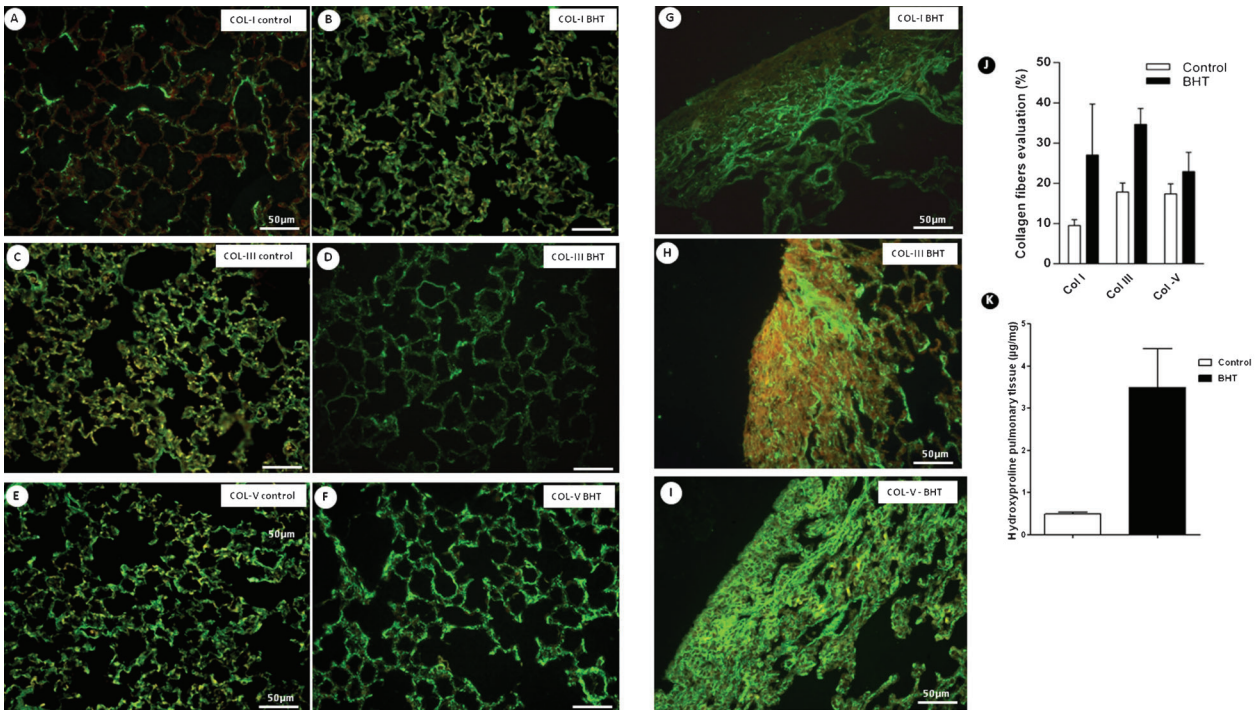

Figure 5. Type I, III, and V collagens from 3-5-di-tert-butyl-4-hydroxytoluene (BHT)-treated mice and the control group at day 28 are shown in histological sections. *A*, *C*, *E*, Control mice showing the normal collagen fibers of types I, III, and V in alveolar interstitium. *B*, *D*, *F*, BHT-treated mice exhibiting a strong green birefringence of collagens I, III, and V in alveolar interstitium of normal areas. *G*, *H*, *I*, BHT-treated mice exhibiting architectural distortion and a diffuse increase of collagens I, III, and V birefringence. *J*, *K*, Effects of BHT on collagen types and hydroxyproline detected by immunofluorescence and biochemistry, respectively. Results are reported as area fraction (%) occupied by collagen fibers and as µg/mg hydroxyproline in alveolar interstitum. Data are reported as means ± SD, n = 20 for the BHT group and n = 10 for the control group. P = 0.05, BHT *vs* control (Student *t*-test). Col: collagen.

components of the telomerase holoenzyme, such as dyskerin, in future studies.

In the present study, the late phase of the experiment was marked by accumulation of extracellular matrix components in lung tissue, predominantly represented by hydroxyproline and collagen types I and III. However, when compared with normal areas, collagen V increased significantly when compared to collagens I and III in scarring areas of UIP. Specifically, collagen V is a minor collagen fraction of hidden molecules that composes heterotypic fibrils together with collagen types I and III. Beyond this aspect, collagen V is highly immunogenic and a cell death inductor (36,37), because it preserves the globular and telopeptide domains. We found a significant direct association between collagen V and AEC2 apoptosis, suggesting that the extensive denudation of the epithelial alveolar capillary membrane resulting from BHT and oxygen cytotoxicity could expose the collagen V epitopes that are normally found hidden inside heterotypic fibrils. This process generates collagen V fragments (neoantigens), which are able to activate the immune system to produce higher amounts of anti-collagen V antibodies and increase the presence of circulating immunocomplexes that, in turn, perpetuate continuous AEC2 aggression and collagen synthesis (38).

In summary, BHT induced increased apoptosis of AEC1. Reepithelization by AEC2 increased telomerase expression, but cytotoxic action by oxygen interfered with AEC proliferation, allowing excessive proliferation of fibroblasts and collagen V. Extensive denudation of the epithelial alveolar capillary membrane by AEC1 apoptosis exposed collagen V epitopes, generating neoantigens, anti-collagen V antibodies, and circulating immunocomplexes, which in turn increased AEC2 apoptosis and collagen V synthesis.

We concluded that telomerase, collagen V fiber density, and apoptosis immunostaining in experimental UIP offers the potential to control the reepithelization of alveolar septa and fibroblast proliferation. Strategies aimed at preventing high levels of collagen V synthesis, or local responses to high levels of cell apoptosis, may have a significant impact on pulmonary fibrosis. To support this conclusion, future studies are necessary at the molecular and genetic levels.

Acknowledgments

We are grateful to Biologist Sandra de Morais Fernezlian from the Laboratory of Immunohistochemistry for her technical assistance. Research supported by FAPESP (#2009/01462-2 and #2008/53022-3).

References

1. Raghu G, Collard HR, Egan JJ, Martinez FJ, Behr J, Brown KK, et al. An official ATS/ERS/JRS/ALAT statement: idiopathic pulmonary fibrosis: evidence-based guidelines for diagnosis and management. *Am J Respir Crit Care Med* 2011; 183: 788-824, doi: 10.1164/rccm.2009-040GL.
2. Katzenstein AL, Myers JL. Idiopathic pulmonary fibrosis: clinical relevance of pathologic classification. *Am J Respir Crit Care Med* 1998; 157: 1301-1315, doi: 10.1164/ajrccm.157.4.9707039.
3. Bringardner BD, Baran CP, Eubank TD, Marsh CB. The role of inflammation in the pathogenesis of idiopathic pulmonary fibrosis. *Antioxid Redox Signal* 2008; 10: 287-301, doi: 10.1089/ars.2007.1897.
4. Meneghin A, Hogaboam CM. Infectious disease, the innate immune response, and fibrosis. *J Clin Invest* 2007; 117: 530-538, doi: 10.1172/JCI30595.
5. Oikonomou N, Harokopos V, Zalevsky J, Valavanis C, Kotanidou A, Szymkowski DE, et al. Soluble TNF mediates the transition from pulmonary inflammation to fibrosis. *PLoS One* 2006; 1: e108, doi: 10.1371/journal.pone.0000108.
6. Todd NW, Luzina IG, Atamas SP. Molecular and cellular mechanisms of pulmonary fibrosis. *Fibrogenesis Tissue Repair* 2012; 5: 11, doi: 10.1186/1755-1536-5-11.
7. Martins V, Valenca SS, Farias-Filho FA, Molinaro R, Simoes RL, Ferreira TP, et al. ATLa, an aspirin-triggered lipoxin A4 synthetic analog, prevents the inflammatory and fibrotic effects of bleomycin-induced pulmonary fibrosis. *J Immunol* 2009; 182: 5374-5381, doi: 10.4049/jimmunol.0802259.
8. Waisberg DR, Barbas-Filho JV, Parra ER, Fernezlian S, de Carvalho CR, Kairalla RA, et al. Abnormal expression of telomerase/apoptosis limits type II alveolar epithelial cell replication in the early remodeling of usual interstitial pneumonia/idiopathic pulmonary fibrosis. *Hum Pathol* 2010; 41: 385-391, doi: 10.1016/j.humpath.2009.08.019.
9. Barbas-Filho JV, Ferreira MA, Sesso A, Kairalla RA, Carvalho CR, Capelozzi VL. Evidence of type II pneumocyte apoptosis in the pathogenesis of idiopathic pulmonary fibrosis (IFP)/usual interstitial pneumonia (UIP). *J Clin Pathol* 2001; 54: 132-138, doi: 10.1136/jcp.54.2.132.
10. Baptista AL, Parra ER, Filho JV, Kairalla RA, de Carvalho CR, Capelozzi VL. Structural features of epithelial remodeling in usual interstitial pneumonia histologic pattern. *Lung* 2006; 184: 239-244, doi: 10.1007/s00408-005-2585-9.
11. Parra ER, Silverio da Costa LR, Ab'Saber A, Ribeiro de Carvalho CR, Kairalla RA, Fernezlian SM, et al. Nonhomogeneous density of CD34 and VCAM-1 alveolar capillaries in major types of idiopathic interstitial pneumonia. *Lung* 2005; 183: 363-373, doi: 10.1007/s00408-005-2548-1.
12. Parra ER, Kairalla RA, de Carvalho CR, Capelozzi VL. Abnormal deposition of collagen/elastic vascular fibres and prognostic significance in idiopathic interstitial pneumonias. *Thorax* 2007; 62: 428-437, doi: 10.1136/thx.2006.062687.
13. Gavrieli Y, Sherman Y, Ben-Sasson SA. Identification of programmed cell death *in situ* via specific labeling of nuclear DNA fragmentation. *J Cell Biol* 1992; 119: 493-501, doi: 10.1083/jcb.119.3.493.
14. Wijsman JH, Jonker RR, Keijzer R, van de Velde CJ, Cornelisse CJ, van Dierendonck JH. A new method to detect apoptosis in paraffin sections: *in situ* end-labeling of fragmented DNA. *J Histochem Cytochem* 1993; 41: 7-12,

doi: 10.1177/41.1.7678025.
15. Bergman I, Loxley R. Two improved and simplified methods for the spectrophotometric determination of hydroxyproline. *Anal Chem* 1963; 35: 1961-1965, doi: 10.1021/ac60205a053.
16. Miller EJ, Rhodes RK. Preparation and characterization of the different types of collagen. *Methods Enzymol* 1982; 82 (Part A): 33-64, doi: 10.1016/0076-6879(82)82059-4.
17. Harlow E, Lane D. *Antibodies: a laboratory manual*. Cold Spring Harbor: Cold Spring Harbor Laboratory; 1988.
18. Hsia CC, Hyde DM, Ochs M, Weibel ER. An official research policy statement of the American Thoracic Society/European Respiratory Society: standards for quantitative assessment of lung structure. *Am J Respir Crit Care Med* 2010; 181: 394-418, doi: 10.1164/rccm.200809-1522ST.
19. Rozin GF, Gomes MM, Parra ER, Kairalla RA, de Carvalho CR, Capelozzi VL. Collagen and elastic system in the remodelling process of major types of idiopathic interstitial pneumonias (IIP). *Histopathology* 2005; 46: 413-421, doi: 10.1111/j.1365-2559.2005.02103.x.
20. Parra ER, Boufelli G, Bertanha F, Samorano LP, Aguiar AC Jr, Costa FM, et al. Temporal evolution of epithelial, vascular and interstitial lung injury in an experimental model of idiopathic pulmonary fibrosis induced by butyl-hydroxytoluene. *Int J Exp Pathol* 2008; 89: 350-357, doi: 10.1111/j.1365-2613.2008.00600.x.
21. Hirai KI, Witschi H, Cote MG. Electron microscopy of butylated hydroxytoluene-induced lung damage in mice. *Exp Mol Pathol* 1977; 27: 295-308, doi: 10.1016/0014-4800(77)90002-8.
22. Adamson IY, Bowden DH. The type 2 cell as progenitor of alveolar epithelial regeneration. A cytodynamic study in mice after exposure to oxygen. *Lab Invest* 1974; 30: 35-42.
23. Evans MJ, Cabral LJ, Stephens RJ, Freeman G. Transformation of alveolar type 2 cells to type 1 cells following exposure to NO2. *Exp Mol Pathol* 1975; 22: 142-150, doi: 10.1016/0014-4800(75)90059-3.
24. Driscoll B, Buckley S, Bui KC, Anderson KD, Warburton D. Telomerase in alveolar epithelial development and repair. *Am J Physiol Lung Cell Mol Physiol* 2000; 279: L1191-L1198.
25. Lee J, Reddy R, Barsky L, Scholes J, Chen H, Shi W, et al. Lung alveolar integrity is compromised by telomere shortening in telomerase-null mice. *Am J Physiol Lung Cell Mol Physiol* 2009; 296: L57-L70, doi: 10.1152/ajplung.90411.2008.
26. Fridlender ZG, Cohen PY, Golan O, Arish N, Wallach-Dayan S, Breuer R. Telomerase activity in bleomycin-induced epithelial cell apoptosis and lung fibrosis. *Eur Respir J* 2007; 30: 205-213, doi: 10.1183/09031936.00009407.
27. Liu T, Chung MJ, Ullenbruch M, Yu H, Jin H, Hu B, et al. Telomerase activity is required for bleomycin-induced pulmonary fibrosis in mice. *J Clin Invest* 2007; 117: 3800-3809.
28. Nozaki Y, Liu T, Hatano K, Gharaee-Kermani M, Phan SH. Induction of telomerase activity in fibroblasts from bleomycin-injured lungs. *Am J Respir Cell Mol Biol* 2000; 23: 460-465, doi: 10.1165/ajrcmb.23.4.3958.
29. Witschi H, Cote MG. Inhibition of butylated hydroxytoluene-induced mouse lung cell division by oxygen: time-effect and dose-effect relationships. *Chem Biol Interact* 1977; 19: 279-289, doi: 10.1016/0009-2797(77)90051-5.
30. Cronkhite JT, Xing C, Raghu G, Chin KM, Torres F, Rosenblatt RL, et al. Telomere shortening in familial and sporadic pulmonary fibrosis. *Am J Respir Crit Care Med* 2008; 178: 729-737, doi: 10.1164/rccm.200804-550OC.
31. Alder JK, Chen JJ, Lancaster L, Danoff S, Su SC, Cogan JD, et al. Short telomeres are a risk factor for idiopathic pulmonary fibrosis. *Proc Natl Acad Sci U S A* 2008; 105: 13051-13056, doi: 10.1073/pnas.0804280105.
32. Armanios MY, Chen JJ, Cogan JD, Alder JK, Ingersoll RG, Markin C, et al. Telomerase mutations in families with idiopathic pulmonary fibrosis. *N Engl J Med* 2007; 356: 1317-1326, doi: 10.1056/NEJMoa066157.
33. Tsakiri KD, Cronkhite JT, Kuan PJ, Xing C, Raghu G, Weissler JC, et al. Adult-onset pulmonary fibrosis caused by mutations in telomerase. *Proc Natl Acad Sci U S A* 2007; 104: 7552-7557, doi: 10.1073/pnas.0701009104.
34. El-Chemaly S, Ziegler SG, Calado RT, Wilson KA, Wu HP, Haughey M, et al. Natural history of pulmonary fibrosis in two subjects with the same telomerase mutation. *Chest* 2011; 139: 1203-1209, doi: 10.1378/chest.10-2048.
35. Hay J, Shahzeidi S, Laurent G. Mechanisms of bleomycin-induced lung damage. *Arch Toxicol* 1991; 65: 81-94, doi: 10.1007/BF02034932.
36. Wilkes DS. Autoimmune responses to grafted lungs: immune responses to a native collagen-Collagen V. *Graft* 2003; 6: 42-49, doi: 10.1177/1522162802239756.
37. Wilkes DS. The role of autoimmunity in the pathogenesis of lung allograft rejection. *Arch Immunol Ther Exp* 2003; 51: 227-230.
38. de Oliveira CC, Velosa AP, Parra ER, Capelozzi VL, Teodoro WR, Yoshinari NH. Histomorphometric analysis of cutaneous remodeling in the early stage of the scleroderma model. *Clinics* 2009; 64: 577-583, doi: 10.1590/S1807-59322009000600014.